Supporting information for: Calcium Phosphate Deposition on Planar and Stepped (101) Surfaces of Anatase TiO_2: Introducing an Interatomic Potential for the TiO_2/Ca-PO_4/Water Interface

Giulia Mancardi,[†,‡] Carlos H. Tamargo,[‡] Umberto Terranova,[‡] and Nora H. De Leeuw[*,‡,†]

†*Department of Chemistry, University College London, 20 Gordon Street, London WC1H 0AJ, UK*

‡*School of Chemistry, Cardiff University, Main Building, Park Place, Cardiff, CF10 3AT, UK*

E-mail: deleeuwn@cardiff.ac.uk

Parameters for the combined force field for calcium phosphate solution in water in contact with an anatase surface

Table S1: Force field parameters from refs.[S1–S5] The shadowed lines report the parameters we obtained applying equations 1-4 in the main article.

Potential parameters				
Atom		Mass (u)		Charge (e)
Ti		47.867		+2.196
O_{Ti}		16.0000		-1.098
Ca		40.078		+2.000
P		30.9738		+5.000
$O_{ph}c$		15.8000		+0.84819
$O_{ph}s$		0.2000		-2.84819
Ow_c		15.8000		+1.25
Ow_s		0.2000		-2.05
Hw		1.0000		+0.4
Core-Shell Spring $\frac{1}{2}k_{c-s}r^2$				
				k_{c-s} $(\frac{eV}{A^2})$
$O_{ph}c$	$O_{ph}s$			74.92038
Ow_c	Ow_s			209.45
Buckingham				$Ae^{-r/\rho} - Cr^{-6}$
		A (eV)	ρ(Å)	C (eV/A^6)
Ti	Ti	31090.38	0.154	5.24
Ti	O_{Ti}	16941.28	0.194	12.57
Ti	$O_{ph}s$	30858.43	0.194	12.57
Ti	Ow_s	1238.72	0.276	6.41
O_{Ti}	O_{Ti}	11771.46	0.234	30.19

O_{Ti}	$O_{ph}s$	6462.53	0.234	30.19
Ca	O_{Ti}	1181.64	0.309227	0.09944
Ca	$O_{ph}s$	2152.3566	0.309227	0.09944
Ca	Ow_s	1186.6	0.297	0.0
P	O_{Ti}	559.98	0.34322	0.03
P	$O_{ph}s$	1020.0	0.34322	0.03
P	Ow_s	465.25	0.34322	0.03
$O_{ph}s$	$O_{ph}s$	22764.3	0.149	27.88
$O_{ph}s$	Ow_s	23987.77	0.213	12.09
$O_{ph}s$	Hw	758.468	0.23	0.0
LJ				$4\epsilon_{ij}[(\frac{\sigma_{ij}}{r_{ij}})^{12} - (\frac{\sigma_{ij}}{r_{ij}})^{6}]$
		σ (Å)	ϵ (eV)	
O_{Ti}	Ow_s	3.446	0.0067	
12-6				$(\frac{A}{r_{ij}})^{12} - (\frac{B}{r_{ij}})^{6}$
		A (eV)	B (eV)	
Ow_s	Ow_s	39344.98	42.15	
nm				$\frac{E_0}{(n-m)}[m(\frac{r_0}{r_{ij}})^{n} - n(\frac{r_0}{r_{ij}})^{m}]$
		E_0 (eV)	n m	r_0(Å)
Ow_s	Hw	0.0555555	9 6	1.817121
schrm				$\frac{k}{2}(\theta_{jik} - \theta_0)^2 exp[-\frac{r_{ij}}{\rho_1} + \frac{r_{ik}}{\rho_2}]$
	k	θ_0	ρ_1	ρ_2
$O_{ph}s$ P $O_{ph}s$	3.3588	109.47	10000000.0	10000000.0

Table S2: Anatase bulk parameters, unit cell volume and bulk modulus obtained (i) after optimization with VASP at the GGA (PBE+D3) level of theory, (ii) optimization with GULP using the Matsui-Akaogi force field[S1] and (iii) experimental values.[S6,S7] Ti−O distances and angles in the optimized bulk are also compared.

	GGA (PBE+D3)	IP[S1]	Experiment
a=b (Å)	3.792	3.770	3.785[S7]
c (Å)	9.560	9.568	9.519[S7]
Volume (Å^3)	137.49	136.00	136.37[S7]
Bulk mod. (GPa)	175	176[a]	178±1[S6]
Ti−O[b] (Å)	1.94	1.93	1.966[S9]
Ti−O (Å)	1.99	1.99	1.937[S9]
O−Ti−O	92.42°	92.49°	92.604°[S9]
O−Ti−O	101.85°	102.02°	102.308°[S9]

[a]Value obtained using the Hill's approximation.[S8]
[b]Anatase has two non equivalent Ti−O bonds.

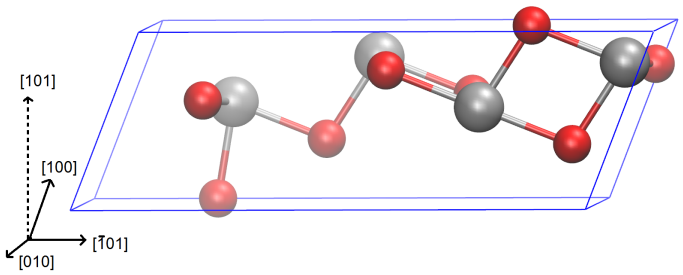

Figure S1: Anatase (101) unit cell. Color key: Ti:grey, O:red

DFT optimization

H_2O adsorption

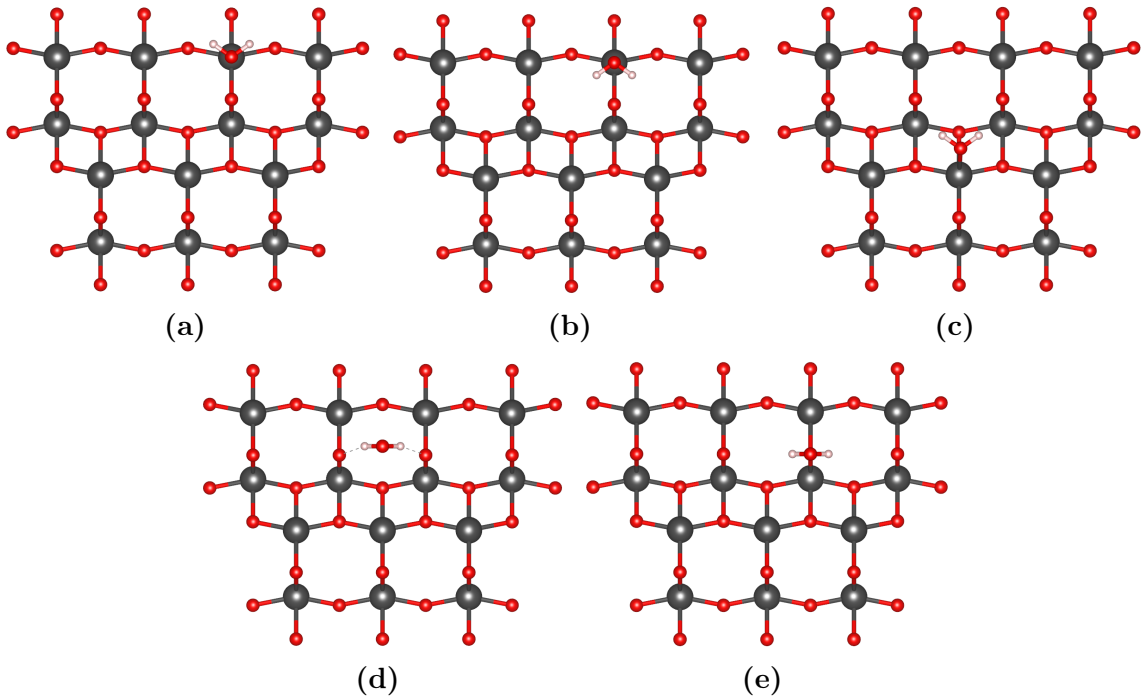

Figure S2: Different starting configurations for the adsorption of a single water molecule on a TiO_2 anatase [101] surface. Color key: Ti:grey, O:red, H:white.

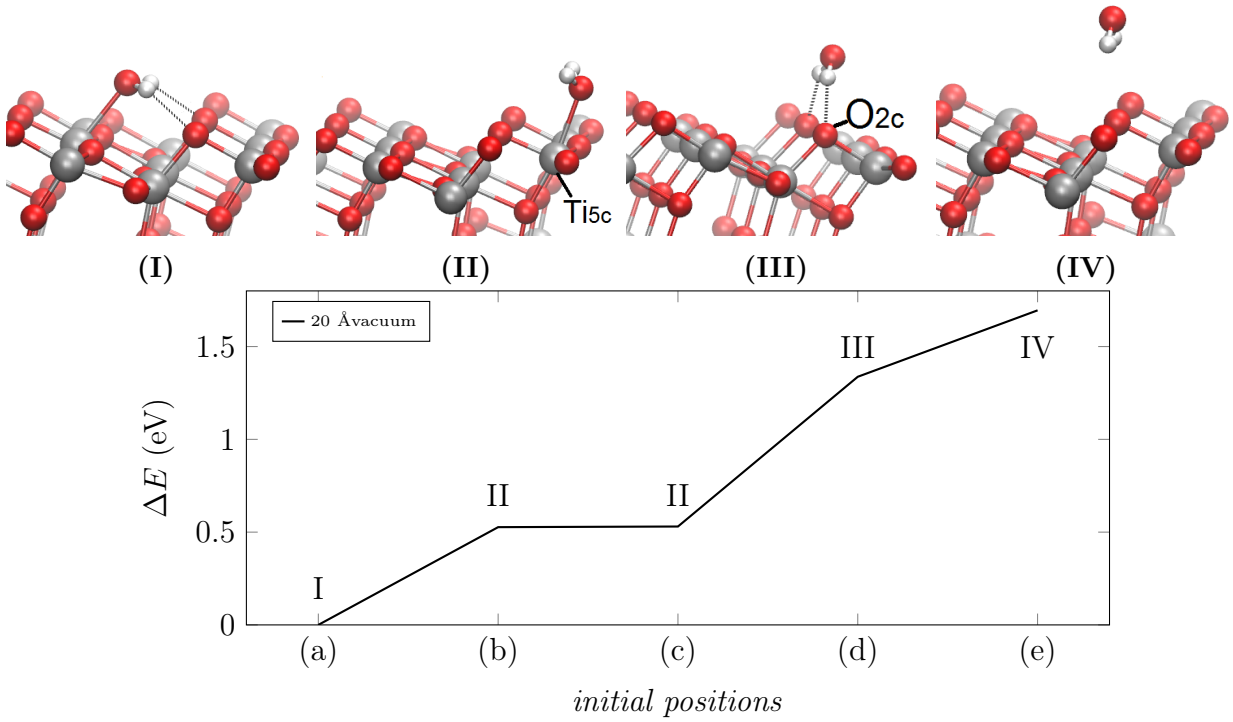

Figure S3: Relative energies after adsorption of two water molecules, one at the top and one at the bottom of the slab, in equivalent positions and a vacuum of 20 Å.

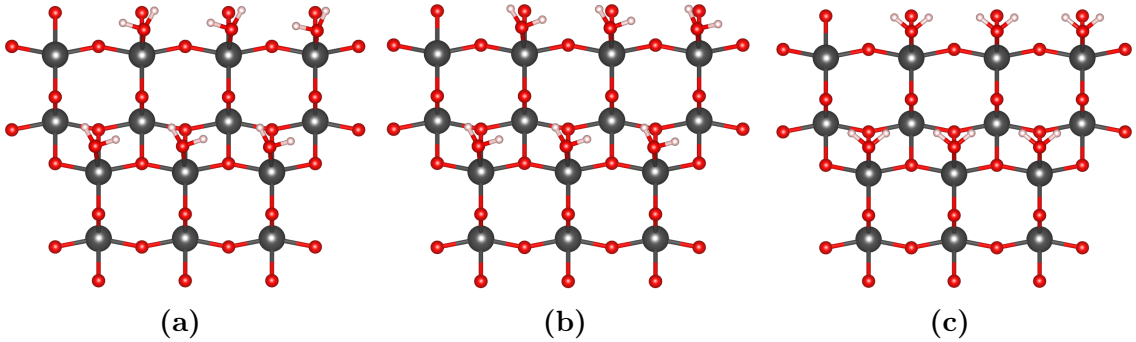

Figure S4: Adsorption of water on a TiO_2 anatase [101] surface, optimized geometries for full coverage. Color key: Ti:grey, O:red, H:white

Ca^{2+} adsorption

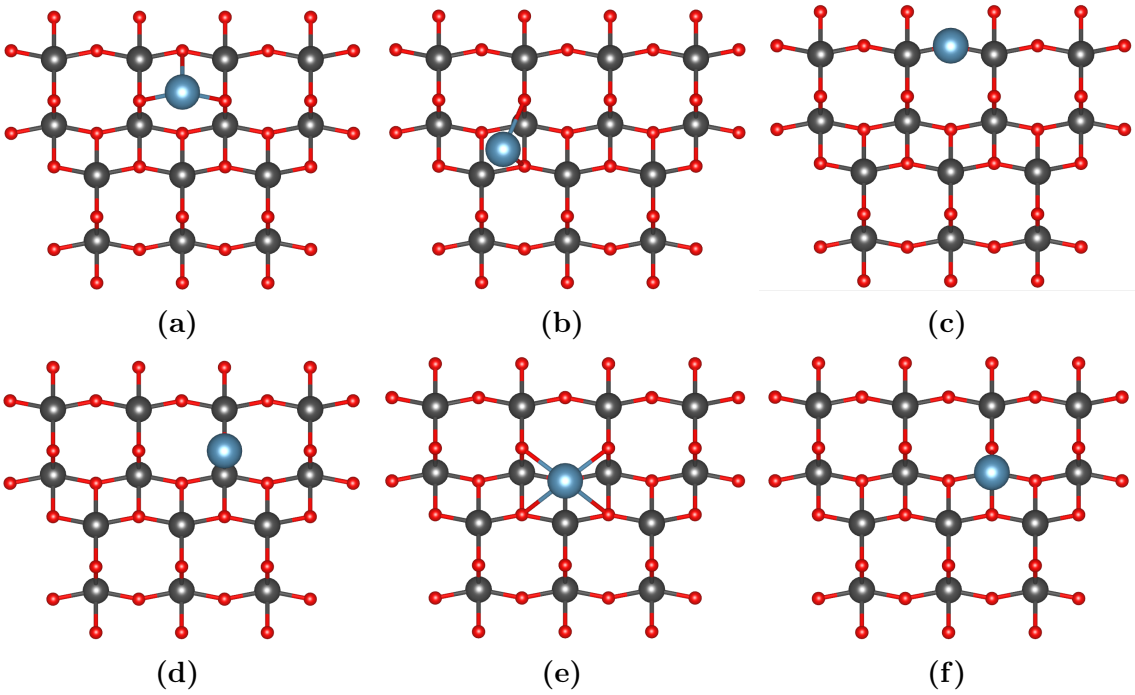

Figure S5: Adsorption of Ca^{2+} on a TiO_2 anatase [101] surface, different starting configurations. Color key: Ti:grey, O:red, Ca:cyan

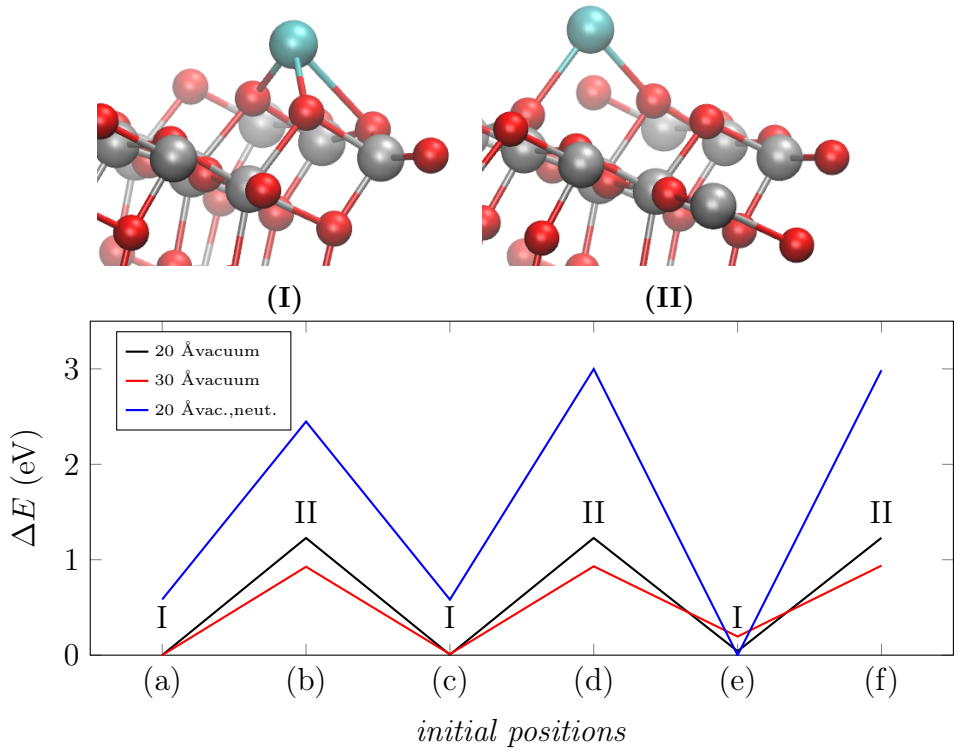

Figure S6: Relative energies after adsorption of (a) two Ca^{2+}, one at the top and one at the bottom of the slab, in equivalent positions and a vacuum of 20 Å (b) two Ca^{2+}, one at the top and one at the bottom of the slab, in equivalent positions and a vacuum of 30 Å and (c) two Ca^{2+}, one at the top and one at the bottom of the slab, in equivalent positions and removal of a Ti^{4+} ion in the frozen core of the slab to make the system neutral. Removing a Ti^{4+} from the slab eliminates the symmetry between the structures I(a) (and I(c)) and the structure I(e).

PO_4^{3-} adsorption

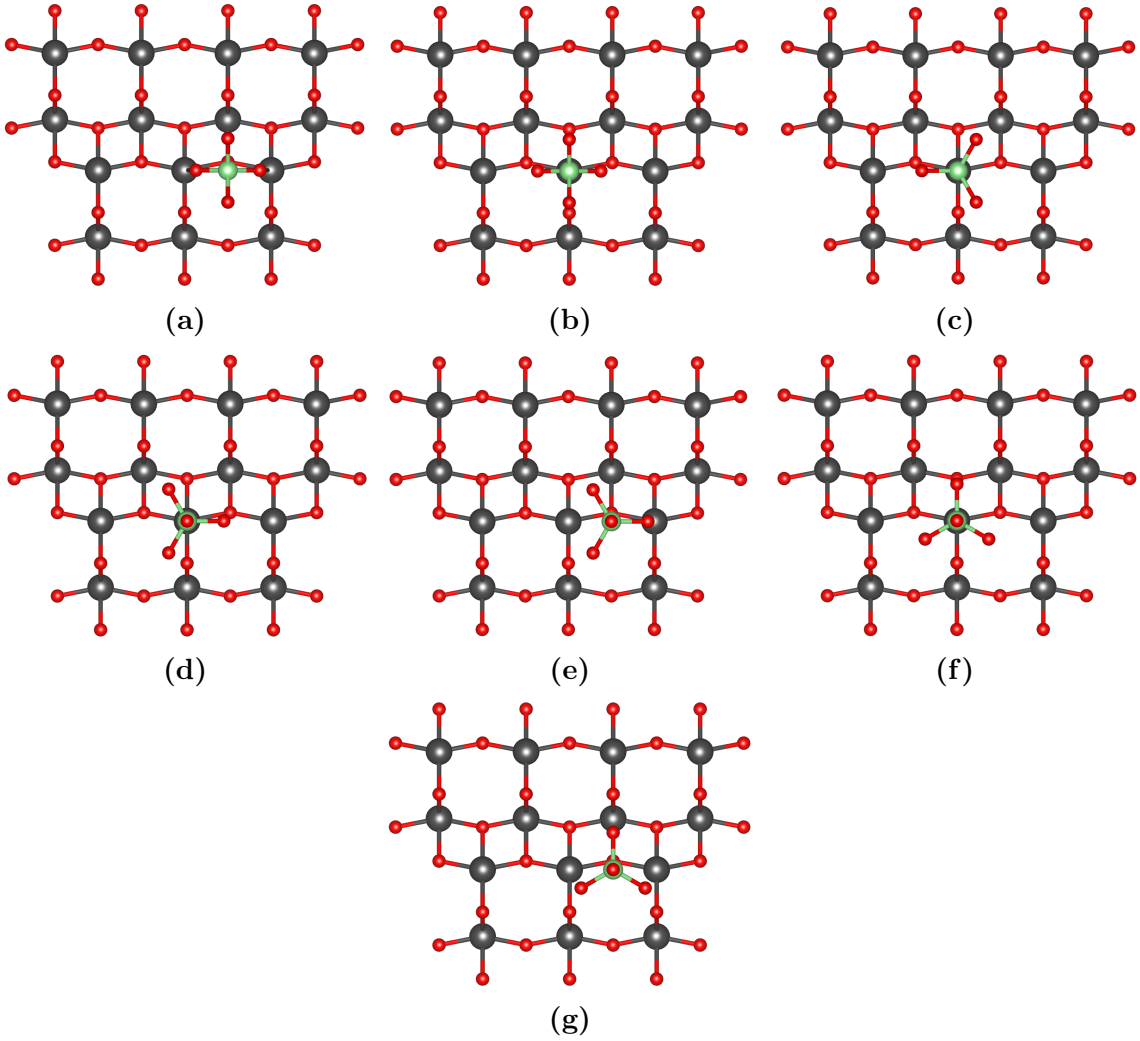

Figure S7: Adsorption of PO_4^{3-} on a TiO_2 anatase [101] surface, different starting configurations.

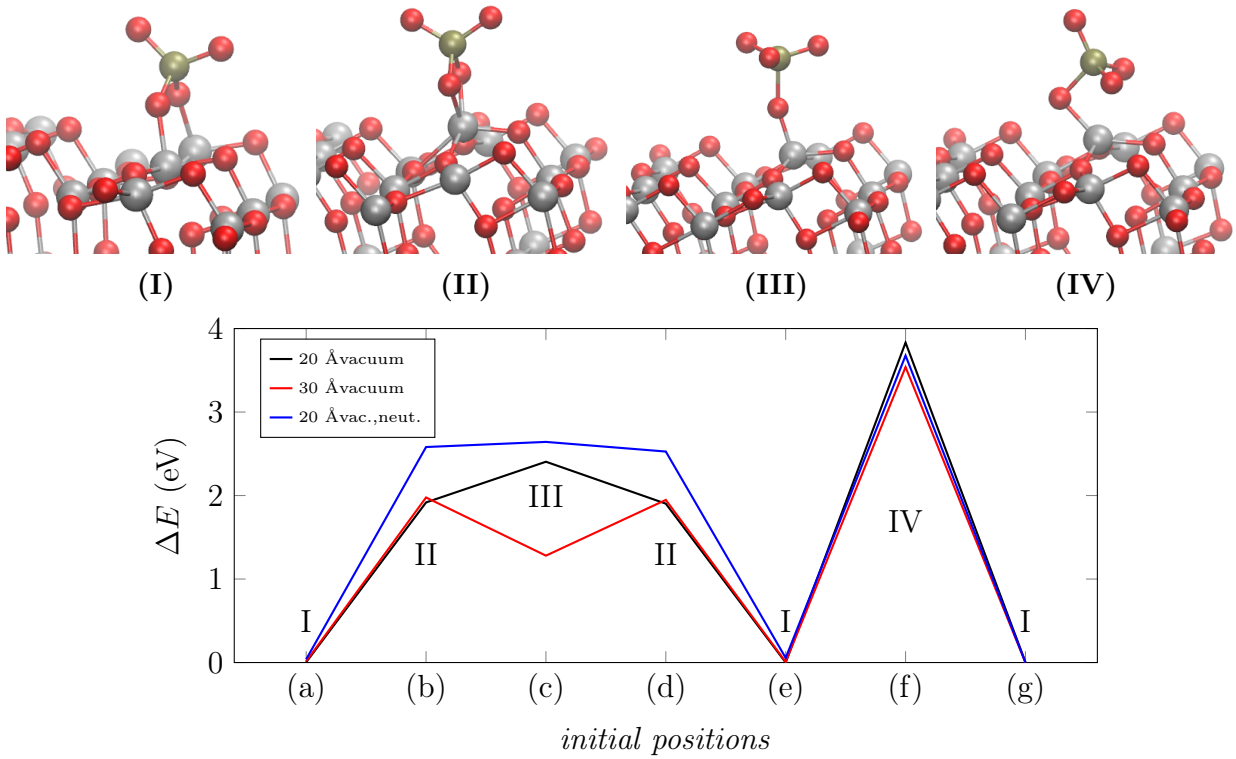

Figure S8: Relative energies after adsorption of (a) two PO_4^{3-}, one at the top and one at the bottom of the slab, in equivalent positions and a vacuum of 20 Å (b) two PO_4^{3-}, one at the top and one at the bottom of the slab, in equivalent positions and a vacuum of 30 Å and (c) two PO_4^{3-}, one at the top and one at the bottom of the slab, in equivalent positions and removal of 3 oxygen ions in the frozen core of the slab to make the system neutral.

Step edges on the anatase (101) surface

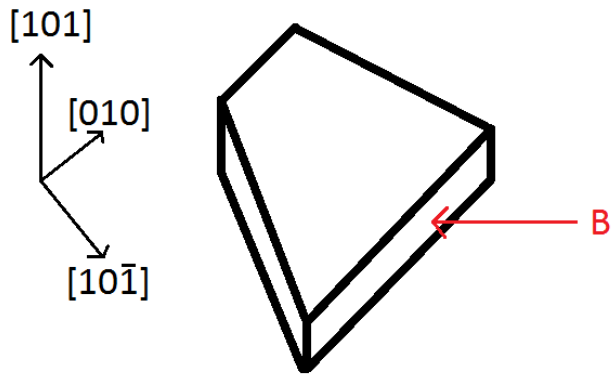

Figure S9: Schematic representation of a trapezoidal island experimentally observed on the anatase (101) surface, with the side of step B indicated by a red arrow.

Water adsorption on anatase surfaces

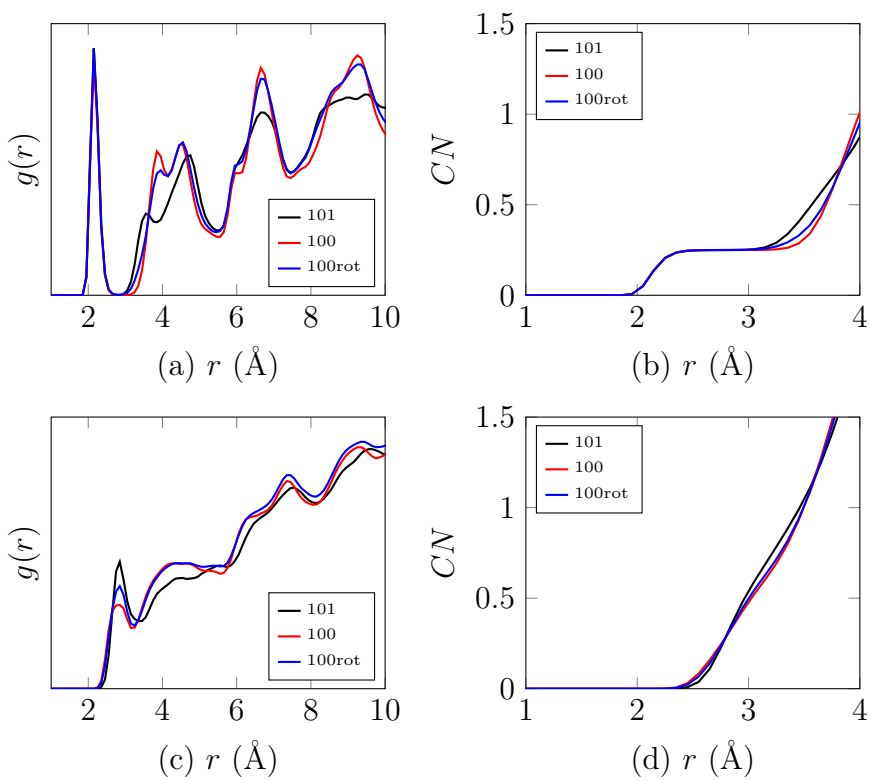

Figure S10: Radial distribution functions and coordination number of (a-b) Ti−O_w and (c-d) Ti−H_w

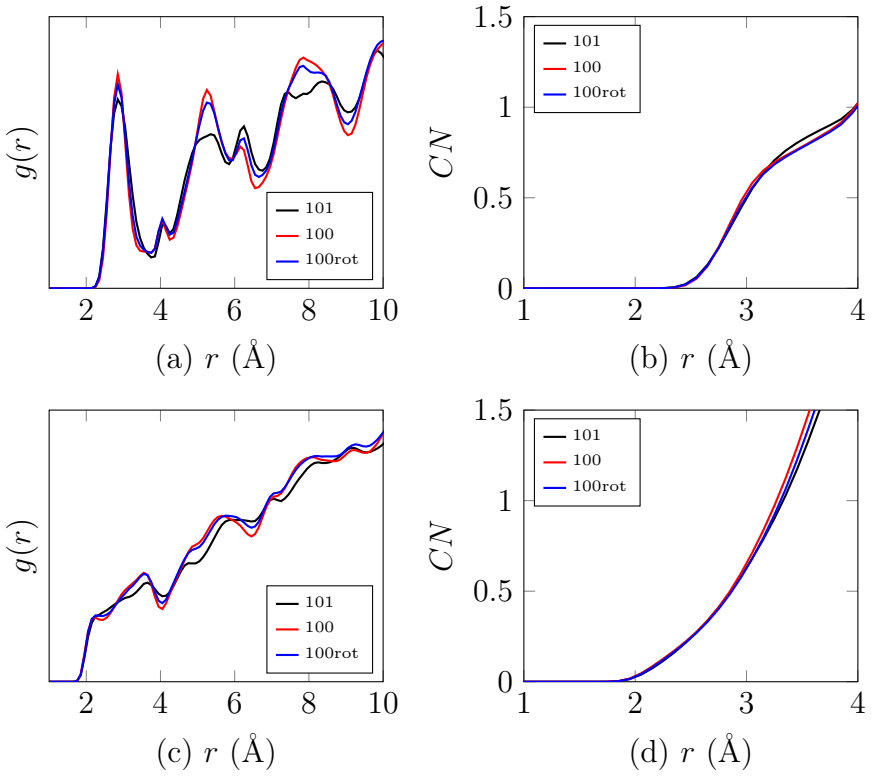

Figure S11: Radial distribution functions and coordination number of (a-b) $O_{Ti}-O_w$ and (c-d) $O_{Ti}-H_w$

Water adsorption on anatase surfaces in presence of calcium and phosphate ions

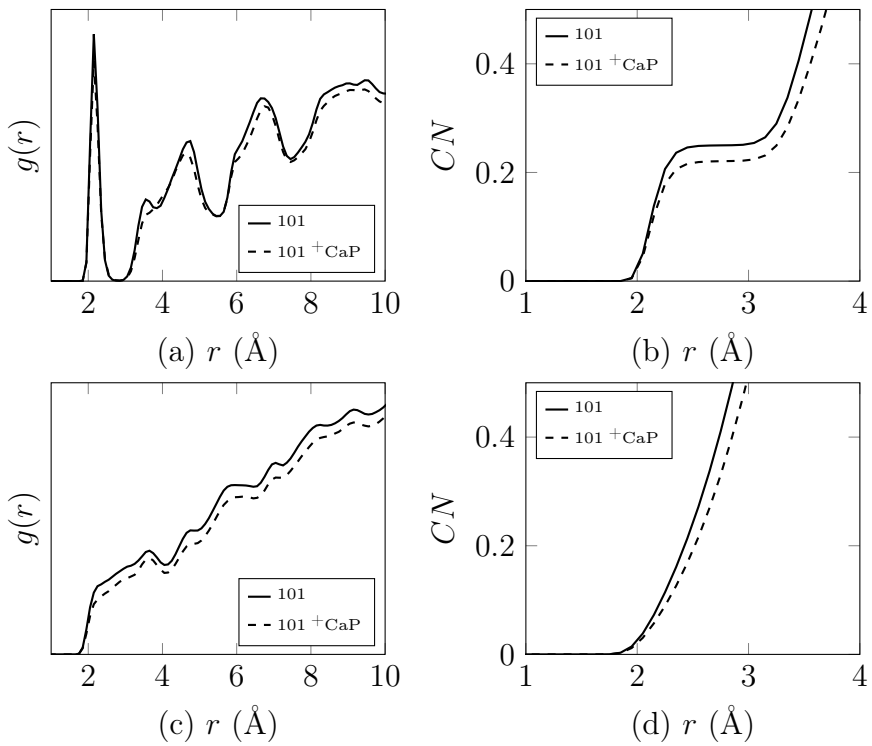

Figure S12: [101] facet: radial distribution functions and coordination number of (a-b) Ti−O_w and (c-d) O_{Ti}−H_w

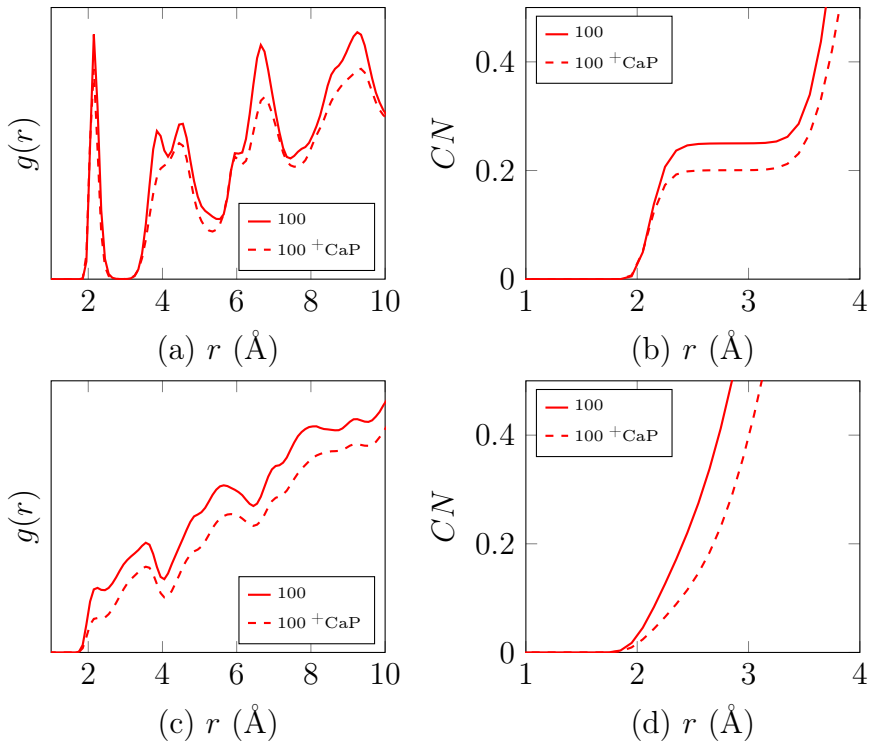

Figure S13: [100] facet: radial distribution functions and coordination number of (a-b) Ti−O_w and (c-d) O_{Ti}−H_w

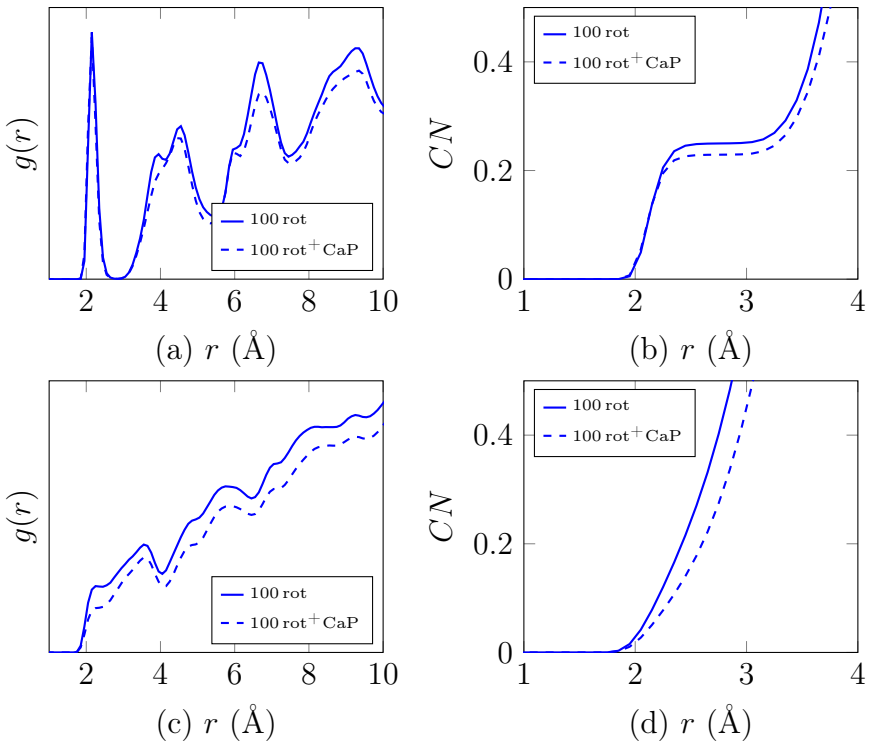

Figure S14: $[100]_{rot}$ surface: radial distribution functions and coordination number of (a-b) $Ti-O_w$ and (c-d) $O_{Ti}-H_w$

Calcium phosphate deposition on Anatase (101), (100) and $(100)_{rot}$ surfaces

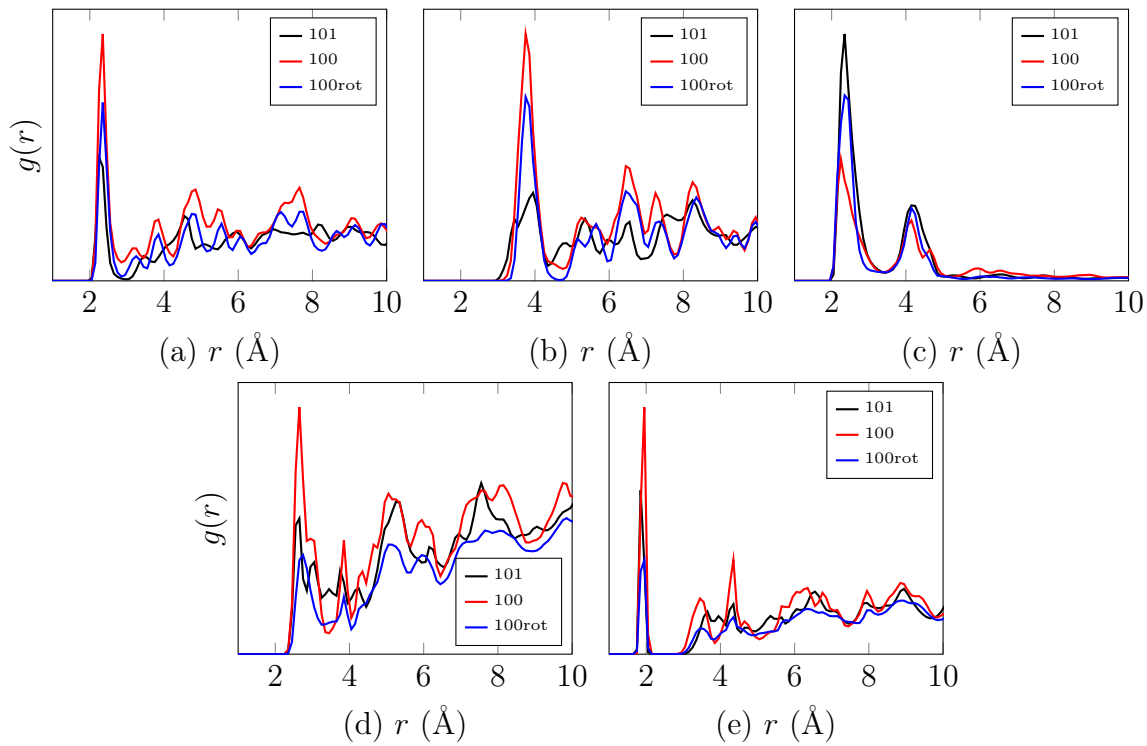

Figure S15: Radial distribution functions of (a) Ca−O_{Ti}, (b) Ca−Ti, (c) Ca−O_{ph}, (d) O_{ph}−O_{Ti} and (e) O_{ph}−Ti.

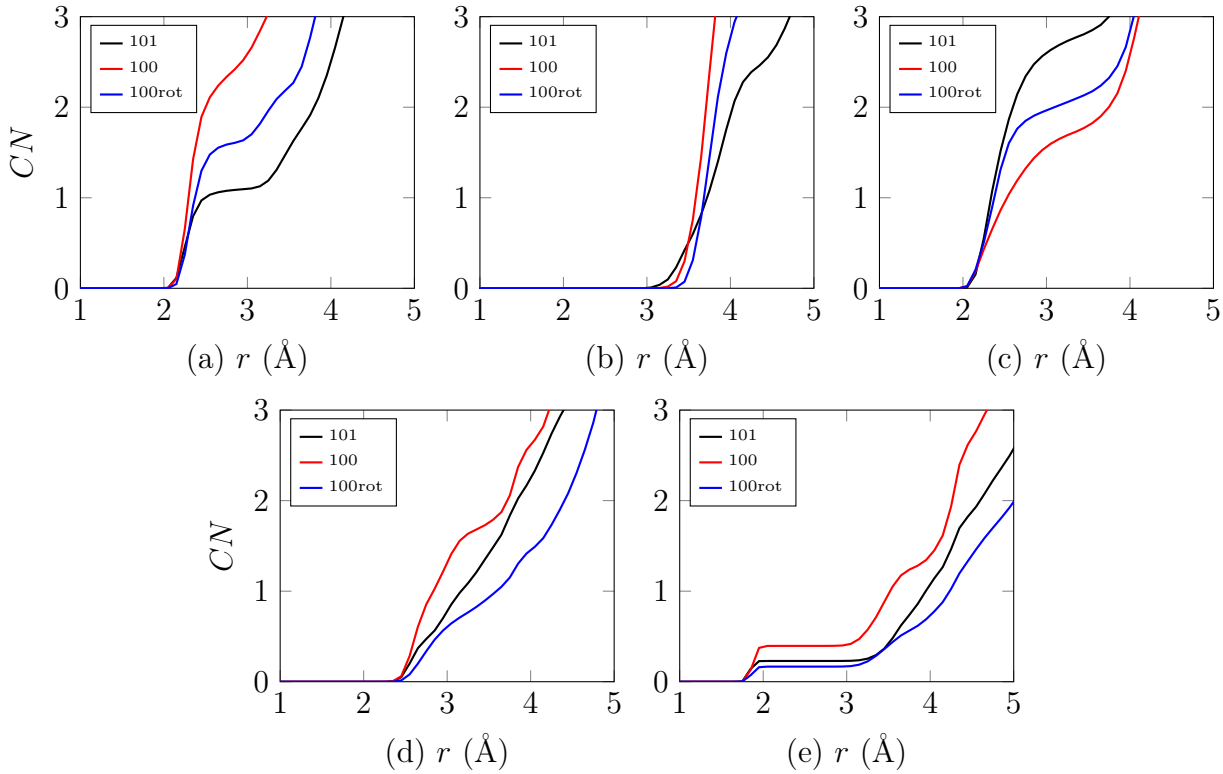

Figure S16: Coordination numbers for (a) Ca−O_{Ti}, (b) Ca−Ti, (c) Ca−O_{ph}, (d) O_{ph}−O_{Ti} and (e) O_{ph}−Ti.

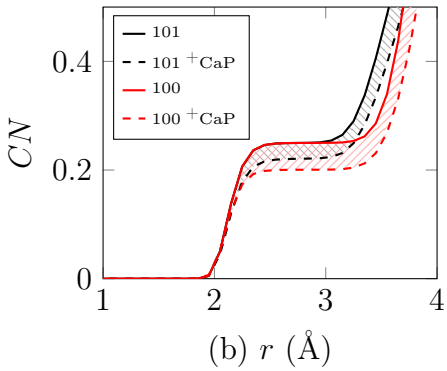

Figure S17: Coordination number of Ti−O_w before (continuous line) and after (dashed line) CaP adsorption. The black lines refer to the (101) and the red lines to the (100) facet.

Comparison of Radial Distribution Functions collected between 0 - 0.25 ns and 0.75 - 1 ns

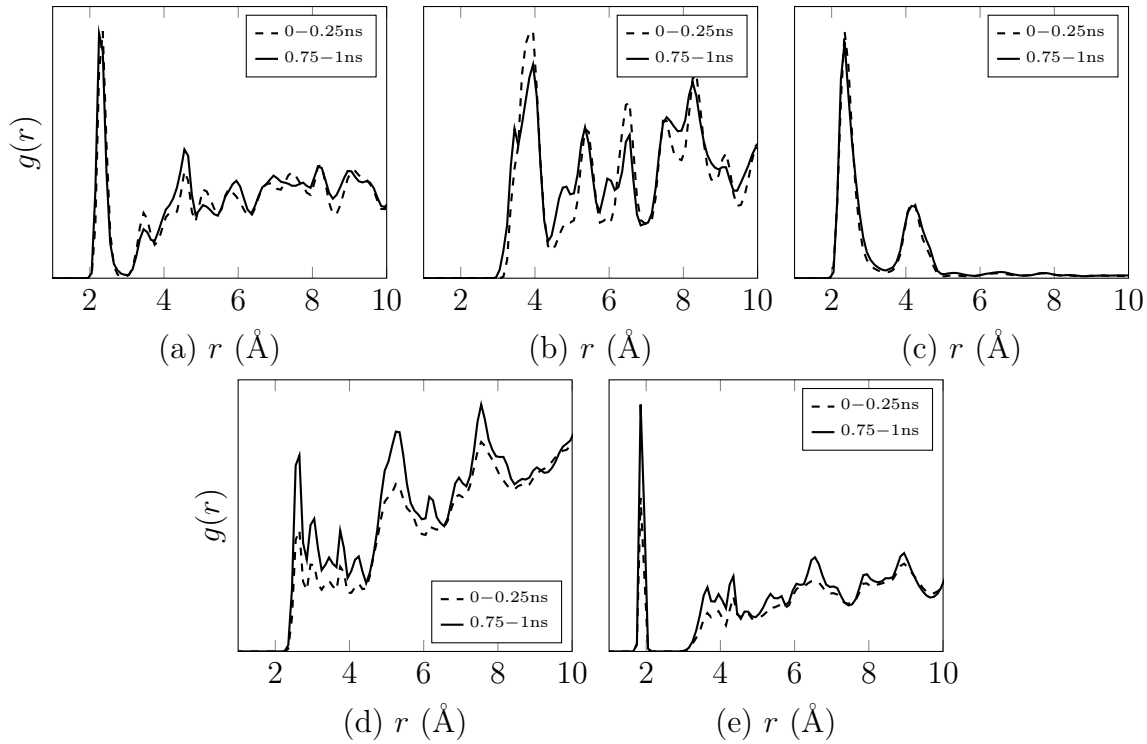

Figure S18: Surface (101): Radial distribution functions of (a) Ca−O_{Ti}, (b) Ca−Ti, (c) Ca−O_{ph}, (d) O_{ph}−O_{Ti} and (e) O_{ph}−Ti. The dashed line refers to rdf collected between 0 and 0.25 ns in an NPT ensemble, whereas the continuous line refers to rdf collected in the final part of the run between 0.75 and 1 ns.

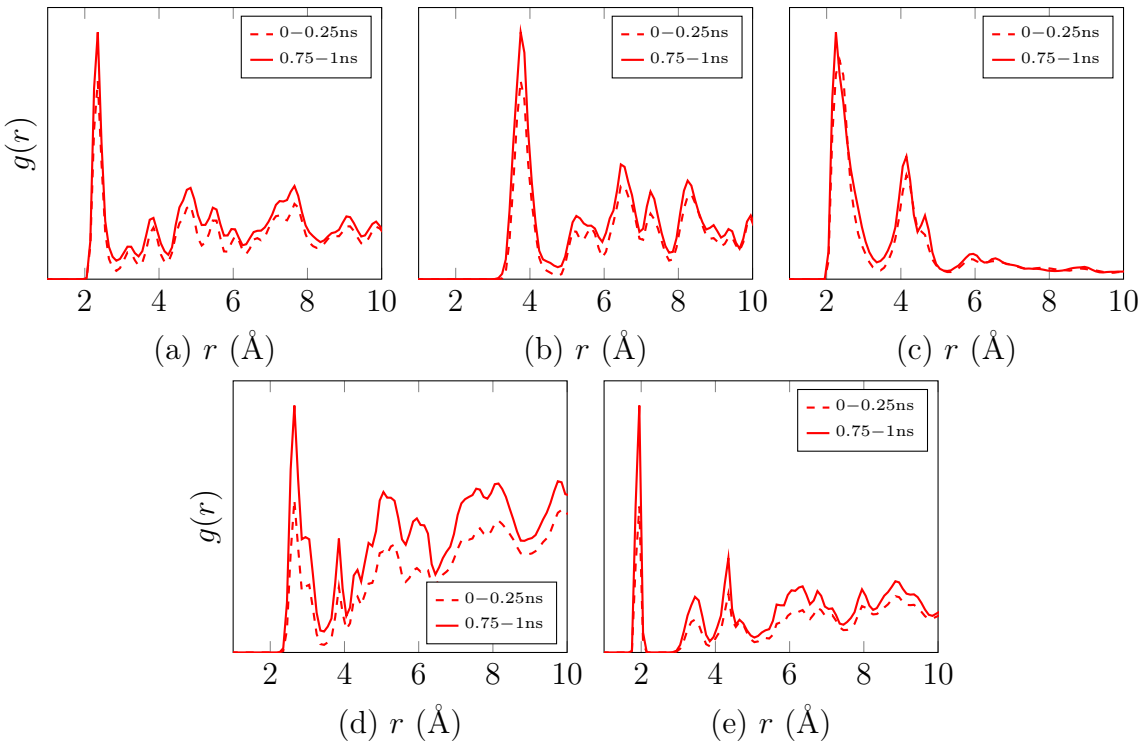

Figure S19: Surface (100): Radial distribution functions of (a) Ca−O_{Ti}, (b) Ca−Ti, (c) Ca−O_{ph}, (d) O_{ph}−O_{Ti} and (e) O_{ph}−Ti. The dashed line refers to rdf collected between 0 and 0.25 ns in an NPT ensemble, whereas the continuous line refers to rdf collected in the final part of the run between 0.75 and 1 ns.

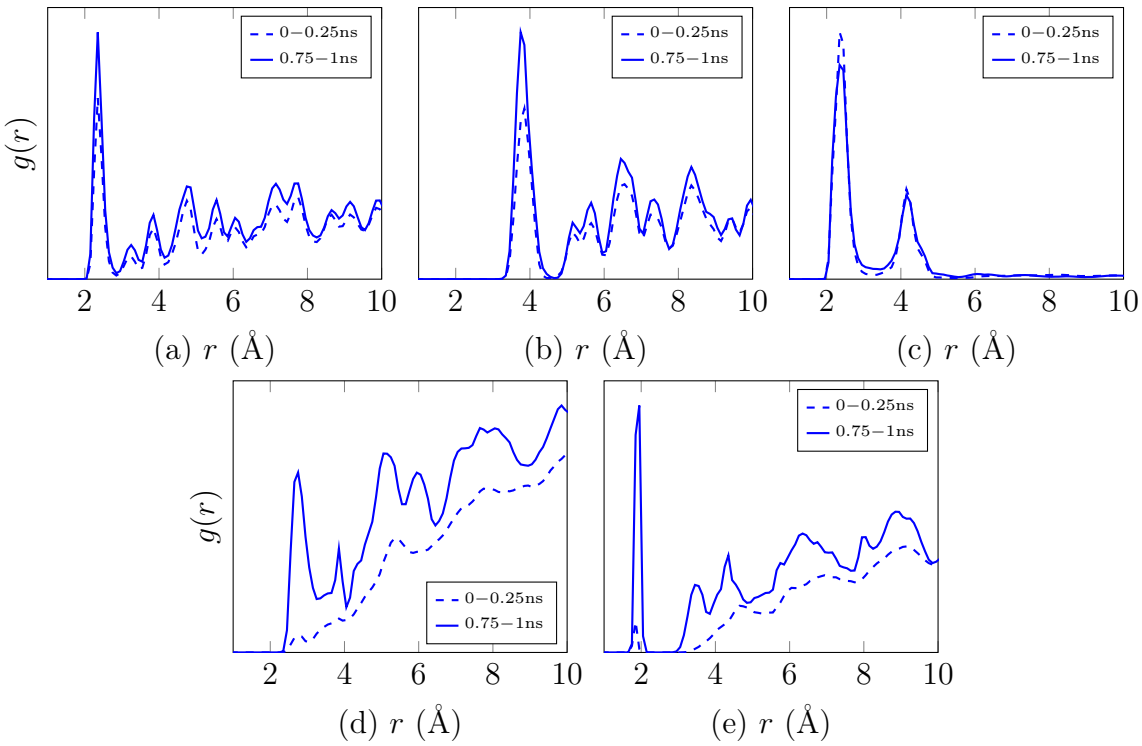

Figure S20: Surface $(100)_{rot}$: Radial distribution functions of (a) Ca−O_{Ti}, (b) Ca−Ti, (c) Ca−O_{ph}, (d) O_{ph}−O_{Ti} and (e) O_{ph}−Ti. The dashed line refers to rdf collected between 0 and 0.25 ns in an NPT ensemble, whereas the continuous line refers to rdf collected in the final part of the run between 0.75 and 1 ns.

Electrostatic Energy, Cell volume and Temperature variation during calcium phosphate deposition on anatase (101), anatase (100) and anatase $(100)_{rot}$ surfaces

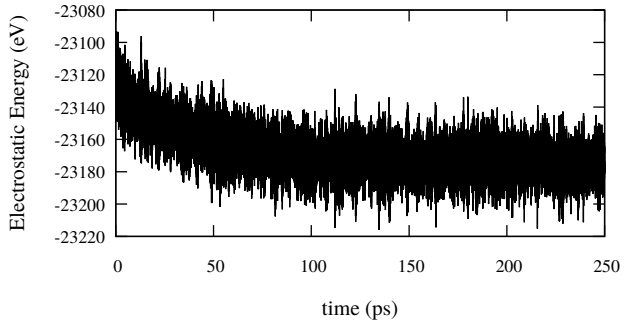

(a)

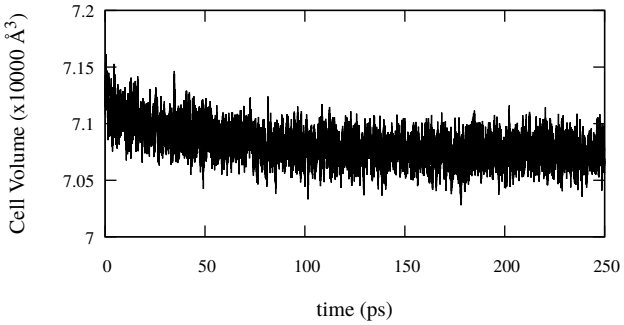

(b)

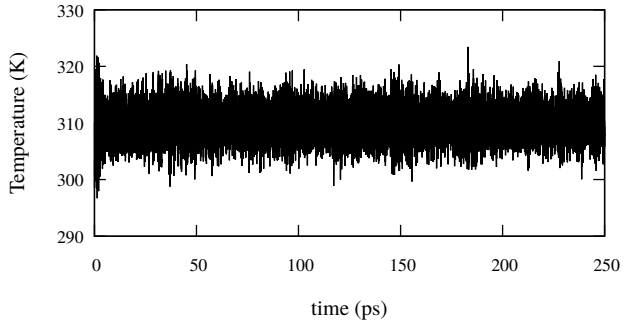

(c)

Figure S21: Calcium phosphate adsorption on TiO_2 anatase (101) surface (a) Electrostatic energy (b) cell volume and (c) temperature variation during the first 0.25 ns of NPT production run

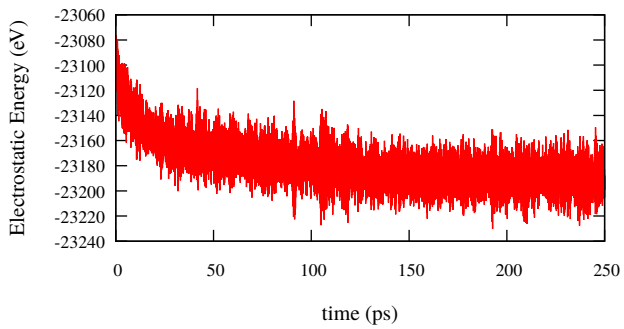

(a)

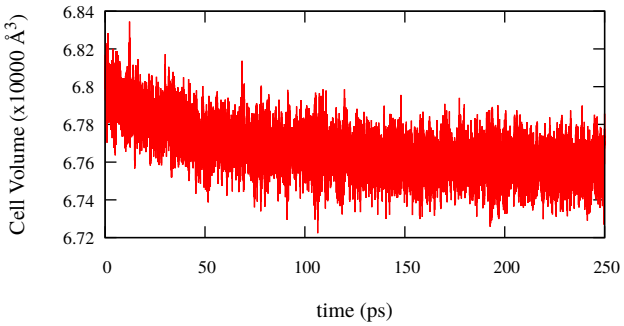

(b)

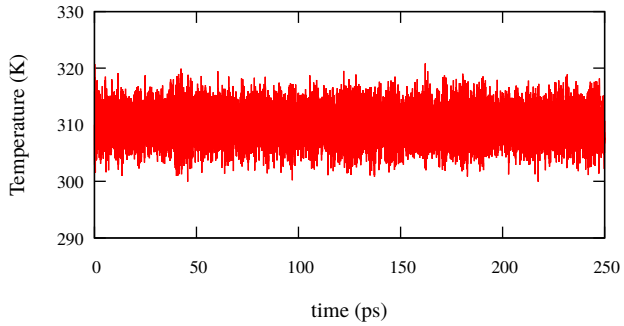

(c)

Figure S22: Calcium phosphate adsorption on TiO_2 anatase (100) surface (a) Electrostatic energy (b) cell volume and (c) temperature variation during the first 0.25 ns of NPT production run

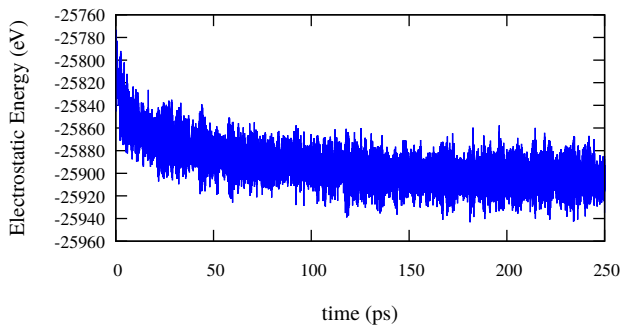

(a)

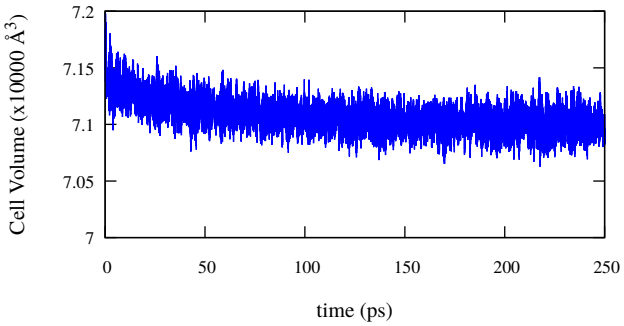

(b)

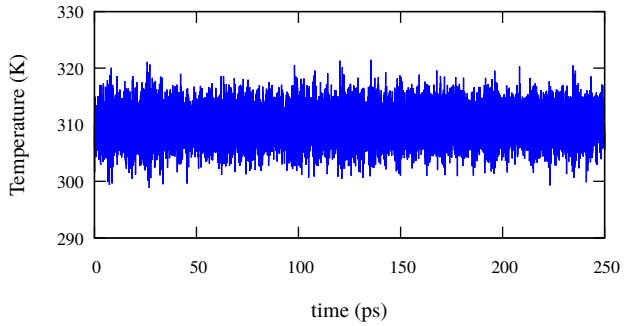

(c)

Figure S23: Calcium phosphate adsorption on TiO_2 anatase $(100)_{rot}$ surface (a) Electrostatic energy (b) cell volume and (c) temperature variation during the first 0.25 ns of NPT production run

References

(S1) Matsui, M.; Akaogi, M. Molecular Dynamics Simulation of the Structural and Physical Properties of the Four Polymorphs of TiO2. *Mol. Simul.* **1991**, *6*, 239–244.

(S2) Alimohammadi, M.; Fichthorn, K. A. A Force Field for the Interaction of Water with TiO2 Surfaces. *J. Phys. Chem. C* **2011**, *115*, 24206–24214.

(S3) Freeman, C. L.; Harding, J. H.; Cooke, D. J.; Elliott, J. A.; Lardge, J. S.; Duffy, D. M. New forcefields for modeling biomineralization processes. *J. Phys. Chem. C* **2007**, *111*, 11943–11951.

(S4) Kerisit, S.; Parker, S. C. Free energy of adsorption of water and calcium on the {1014} calcite surface. *J. Am. Chem. Soc.* **2004**, *126*, 10152–10161.

(S5) Ainsworth, R. I.; Di Tommaso, D.; Christie, J. K.; de Leeuw, N. H. Polarizable force field development and molecular dynamics study of phosphate-based glasses. *J. Chem. Phys.* **2012**, *137*, 234502.

(S6) Swamy, V.; Dubrovinsky, L. S. Bulk modulus of anatase. *J. Phys. Chem. Solids* **2001**, *62*, 673–675.

(S7) Rezaee, M.; Mousavi Khoie, S. M.; Liu, K. H. The role of brookite in mechanical activation of anatase-to-rutile transformation of nanocrystalline TiO2: An XRD and Raman spectroscopy investigation. *CrystEngComm* **2011**, *13*, 5055–5061.

(S8) Hill, R. The Elastic Behaviour of a Crystalline Aggregate. *Proc. Phys. Soc. Section A* **1952**, *65*, 349–354.

(S9) Samsonov, G. *The Oxide Handbook*; IVI/Plenum Press: New York, 1982.